SCIENCE CHINA
Information Sciences

• RESEARCH PAPER •

June 2019, Vol. 62 062403:1–062403:11
https://doi.org/10.1007/s11432-018-9503-9

Simulation of a high-performance enhancement-mode HFET with back-to-back graded AlGaN layers

Fu PENG, Chao YANG, Siyu DENG, Dongya OUYANG, Bo ZHANG, Jie WEI* & Xiaorong LUO*

State Key Laboratory of Electronic Thin Films and Integrated Devices, University of Electronic Science and Technology of China, Chengdu 610054, China

Received 9 February 2018/Revised 21 April 2018/Accepted 21 June 2018/Published online 16 January 2019

Abstract A novel three-dimensional hole gas (3DHG) enhancement-mode (E-mode) heterostructure field-effect transistor (HFET) is proposed and investigated. It features back-to-back graded AlGaN (BGA) barrier layers consisting of a positive-graded AlGaN layer and a negative-graded AlGaN layer, which form polarization gradient and subsequently induce the three-dimensional electron gas (3DEG) and 3DHG in the positive- and negative-graded AlGaN layers, respectively. The source and drain are located at the same side of the metal-insulator-semiconductor (MIS) trench gate, and the source is in contact with the HfO_2 gate insulator. First, the on-state current is significantly improved owing to the high-density 3DEG in the positive-graded AlGaN. Next, the vertical conductive channel between the source and 3DEG is blocked by the 3DHG, thereby realizing the E-mode. The threshold voltage ($V_{\rm th}$) can be modulated by a partial doping conductive channel. Subsequently, a high breakdown voltage (BV) is obtained, because the polarization junction formed by the polarization charges assists in depleting the drift region in the off-state. Next, the BGA-HFET is smaller than the conventional HFET (Con-HFET) owing to the special location of the source. The BV of the proposed HFET sharply increases to 919 V from 39 V of the Con-HFET with the same gate-drain spacing, and the saturation drain current is increased by 103.5%.

Keywords graded AlGaN, 3DHG-3DEG, large on-state current, high voltage, enhancement mode

Citation Peng F, Yang C, Deng S Y, et al. Simulation of a high-performance enhancement-mode HFET with back-to-back graded AlGaN layers. Sci China Inf Sci, 2019, 62(6): 062403, https://doi.org/10.1007/s11432-018-9503-9

1 Introduction

Owing to their superior material properties and great prospect in the next-generation microwave power amplifiers and high-voltage switches applications, GaN-based heterostructure field-effect transistors (HFETs) have attracted substantial research attention [1–4]. The two-dimensional electron gas (2DEG) is the foundation of the abrupt GaN HFETs [5]. Consequently, the conventional AlGaN/GaN HFET (Con-HFET) is of depletion mode (D-mode) intrinsically although the enhancement mode (E-mode) is desired strongly for power electronic applications. To achieve an E-mode operation, numerous techniques have been proposed [6–11]. These conventional E-mode techniques are realized by depleting the 2DEG under the gate, which will inevitably lead to the contradiction between high threshold voltage ($V_{\rm th}$) and large saturation drain current ($I_{\rm d,sat}$).

The critical breakdown electric field (E-field) of GaN is ten times that of silicon [12]. However, the breakdown voltage (BV) of GaN HFETs is far lower than its theoretical limit currently. One important reason is that the E-field crowding at the gate edge leads to premature breakdown in the off-state. To

* Corresponding author (email: weijieuestc@gmail.com, xrluo@uestc.edu.cn)

address this issue, several technologies have been employed, including the field plate (FP) [13], RESURF technique [14], and polarization junction concept [15, 16]. However, the introduction of the FP will increase the parasitic capacitance. The other methods may induce significant negative impact on the on-state performance.

The graded AlGaN/GaN heterostructures have attracted much interest over the last decades [17–23]. Unlike the conventional abrupt AlGaN/GaN heterostructures, the 2DEG formed at the AlGaN/GaN interface extends to a three-dimensional electron profile across the graded AlGaN region significantly. Li et al. [21] reported a polarization-induced pn-junction with neither the p-type dopant nor the n-type dopant, and its breakdown voltage (34.1 V) was almost as high as the regularly doped GaN pn-junction (36.7 V). Fang et al. [22] demonstrated a D-mode polarization-doped field-effect transistor (PolFET) based on graded AlGaN epilayers. However, limited work has been performed on three-terminal GaN POWER devices with symmetrically graded AlGaN.

Herein, a novel three-dimensional hole gas (3DHG) E-mode HFET with back-to-back graded AlGaN (BGA-HFET) is proposed and its on-state as well as off-state electrical performances are investigated by simulation. The proposed BGA-HFET features the symmetrically graded AlGaN structure and special location of the source. The three-dimensional electron gas (3DEG) and 3DHG are induced in the positive- and negative-graded AlGaN layers, respectively. Benefiting from the assisted depletion effect of polarization junction and the high-concentration 3DEG in the positive-graded AlGaN, the BV and $I_{\rm d,sat}$ of the BGA-HFET are significantly improved. A new E-mode operation is also achieved by utilizing the 3DHG to block the vertical conductive channel between the source and 3DEG. In addition, an adjustable $V_{\rm th}$ and large transconductance are obtained in the new structure.

2 Device structure and mechanism

Figure 1(a) is the schematic cross section of the proposed BGA-HFET [24]. The HFET features back-to-back graded AlGaN barrier layers. The aluminum (Al) composition linearly increases from 0 to $x_{\rm Al}$ for the positive-graded AlGaN and subsequently decreases from $x_{\rm Al}$ to 0 through the negative-graded AlGaN in the vertical direction, as shown in Figure 1(b). The $x_{\rm Al}$ represents the maximum Al composition at the positive-/negative-graded AlGaN interface, and d represents the thickness of each graded AlGaN layer. The GaN-top layer is disposed on the negative-graded AlGaN. The MIS trench gate extends into the GaN buffer layer. The source and drain located at the same side of the MIS trench gate form an Ohmic contact with the GaN-top layer and positive-graded AlGaN layer, respectively. The source is in contact with the HfO_2 gate insulator to form a vertical channel. The N region under the source is used to regulate $V_{\rm th}$, with doping concentration $N_{\rm s}$. The drain and the negative-graded AlGaN are isolated by a gap to avoid the migration of the hole leakage current from the drain to the gate. The X and Y directions are shown in Figure 1(a).

Unlike the abrupt AlGaN/GaN heterojunction, a linearly graded AlGaN layer spreads the polarization sheet charges into three-dimensional polarization volume charges as demonstrated in Figure 1(c), and is expressed by $N_D^{\rm Pol}(z) = \nabla \cdot P = [P(z_0) - P(0)]/z_0$ as mentioned in [17]. Hence, to neutralize the fixed polarization charges, the 3DEG and 3DHG are induced in the positive- and negative-graded AlGaN layers, respectively.

The 3DHG blocks the vertical conductive channel between the source and 3DEG, thereby achieving a new E-mode operation. It is different from the traditional E-mode methods by depleting the 2DEG under the gate, which demands a tradeoff relationship between a high $V_{\rm th}$ and large $I_{\rm d,sat}$. For the BGA-HFET, in the on-state, the 3DHG along the sidewall of the trench gate is depleted and the electrons accumulation layer (EAL) is subsequently formed, providing a source-EAL-3DEG electron current path. The on-state current is prominently improved owing to the high-concentration 3DEG in the positive-graded AlGaN. It is noteworthy that the gradient of the Al composition is symmetrical in the positive- and negative-graded AlGaN. Consequently, the polarization junction meets the charge balance condition and has a similar effect as a RESURF or superjunction (SJ) in silicon [25, 26]. During the off-state period, a flat E-field

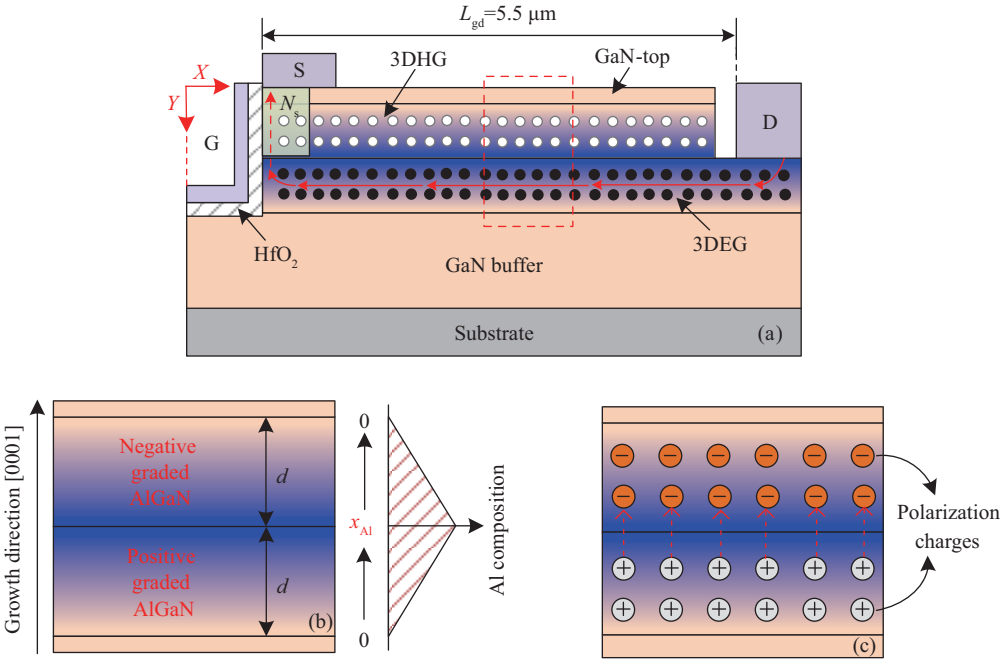

Figure 1 (Color online) (a) Schematic cross section of the BGA-HFET in the on-state; (b) expansion of back-to-back graded AlGaN and diagram of Al composition; (c) polarization charges created by graded AlGaN.

distribution can be achieved between the trench gate and drain owing to the assisted depletion effect caused by the polarization junction. Consequently, the BV of the BGA-HFET is significantly enhanced.

The back-to-back graded AlGaN could be epitaxially grown by metal organic chemical vapor deposition (MOCVD) or molecular beam epitaxy (MBE) on the Ga-face (0111) GaN buffer layer [20,21,27,28]. The feasible processing steps of the BGA-HFET will be discussed at the end herein. The HfO_2 thickness is 10 nm, the gate length (L_g), and source length (L_s) are both 0.5 μm; the drain length (L_d) is 1 μm, and the gate-drain spacing (L_{gd}) is 5.5 μm. The thickness of the GaN-top layer with an n-type doping concentration of 1×10^{15} cm^{-3} is 20 nm. Further, a 1.5-μm-thick GaN slightly n-type doped (N_B=1×10^{15} cm^{-3}) buffer layer was grown on the sapphire substrate. The net acceptor (deep level) density in the buffer layer is set to be 1.5×10^{16} cm^{-3} and the energy level is 0.45 eV below the conduction band minimum [29]. The electron mobility at the AlGaN/GaN buffer layer heterointerface is assumed to be 925 cm^2/(V·s) for the BGA-HFET and PolFET [19], while 1500 cm^2/(V·s) for the Con-HFET, and 300 cm^2/(V·s) at the MIS trench gate interface for the three devices [30].

The physical mechanism is analyzed based on the 2D Sentaurus TCAD by Synopsys. The hydrodynamic transport equations are adopted in simulations. Several important physical models such as the avalanche ionization, bandgap narrowing, high field saturation, doping dependence, and Shockley-Read-Hall and spontaneous polarizations are also accounted.

3 Result and discussion

Figure 2 shows the electron density distributions of the BGA-HFET at different V_g. The 3DEG and 3DHG are induced in the positive- and negative-graded AlGaN layers, respectively. In this paper, d = 100 nm and x_{Al} = 0.4 are fixed unless otherwise specified, and the doping concentration of N_s is set as 8×10^{16} cm^{-3}. In Figure 2(a), at V_g = 0 V, the electron current path between the source and 3DEG is effectively blocked by the 3DHG, thereby realizing the E-mode. However, when V_g = 4 V, the 3DHG along the trench gate side is depleted and EAL is formed, as demonstrated by the blue dash rectangle in Figure 2(b); thus, the electrons could flow via the source-EAL-3DEG current path.

Figure 3 illustrates the conduction band profile along the gate sidewall at different V_g. Y = 200 nm is

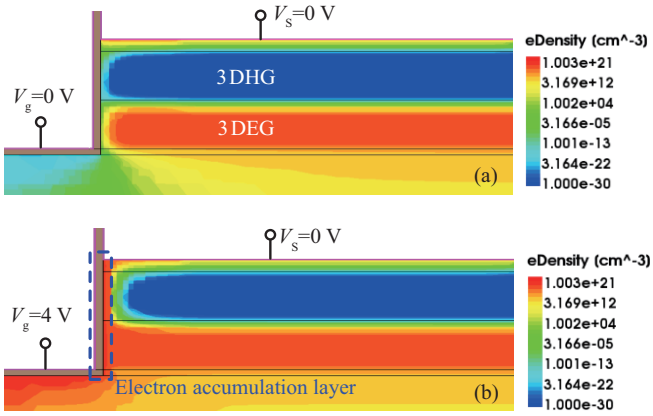

Figure 2 (Color online) Electron density distributions of BGA-HFET around the MIS trench gate and source region at (a) $V_g = 0$ V and (b) $V_g = 4$ V.

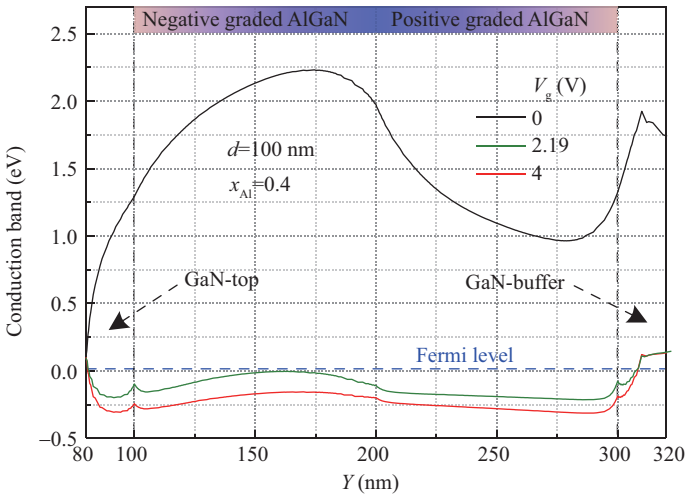

Figure 3 (Color online) Conduction band profile along the gate sidewall at different V_g.

the positive-/negative-graded AlGaN interface. At $V_g = 0$ V, the conduction band of the whole positive-/negative-graded AlGaN is above the Fermi level, indicating no accumulated electron and no current path. With the increasing gate voltage, the conduction band is pulled down. When $V_g = 2.19$ V, the peak of the conduction band keeps flushing with the Fermi level. When $V_g > V_{th}$ (e.g., $V_g = 4$ V), the conduction band is lower than the Fermi level, the EAL is formed, connecting the source to the 3DEG electron current path.

A PolFET and abrupt AlGaN/GaN heterostructure (i.e., the Con-HFET) are simulated for comparison, and their schematic cross sections are shown in Figure 4(a) and (b), respectively. The Con-HFET and PolFET have the same L_g, L_d, and L_{gd} as the BGA-HFET. In the BGA-HFET, the conduction band in most of the positive-graded AlGaN and the valence band in the negative-graded AlGaN are slightly lower than the Fermi level. Consequently, in the Y direction, the BGA-HFET not only has a high-density 3DEG ($\sim 2\times10^{18}$ cm^{-3}) in the wide range of the positive-graded AlGaN, but also has an equal profile of 3DHG through the negative-graded AlGaN, as shown in Figure 5(a). To compare the PolFET with the BGA-HFET, the 200-nm-thick back-to-back graded AlGaN for the BGA-HFET is replaced by a 100-nm-thick positive-graded AlGaN. The potential well of the conduction band of the PolFET is shallow with a wide distance. Consequently, a constant 3DEG across the graded AlGaN is generated as shown in Figure 5(b). However, a deep well-defined triangular potential well and high 2DEG density (maximum value $\sim 4\times10^{19}$ cm^{-3}) are observed in the Con-HFET structure owing to the polarization discontinuity, as shown in Figure 5(c).

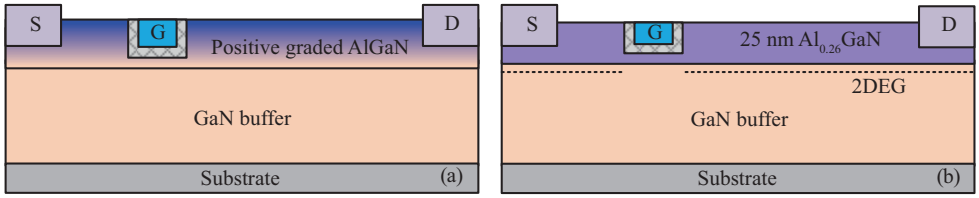

Figure 4 (Color online) Schematic cross section of the (a) PolFET and (b) Con-HFET.

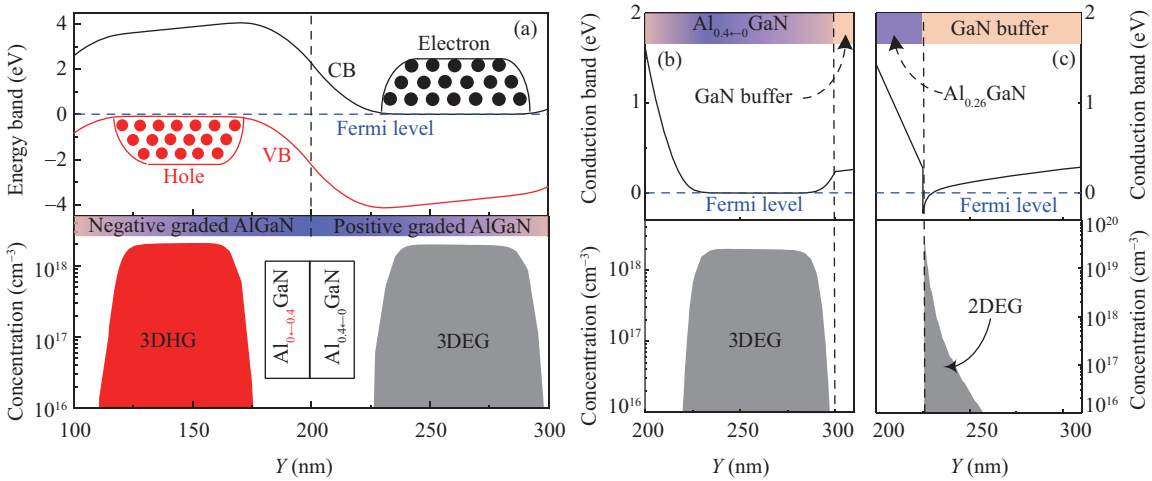

Figure 5 (Color online) Energy band profiles and carrier concentration distributions of (a) BGA-HFET, (b) PolFET, (c) Con-HFET.

Figure 6 shows the transfer characteristics and transconductance (g_m) at $V_{\rm d}$ = 0.5 V. The PolFET and Con-HFET are designed to achieve the same $V_{\rm th}$ as the BGA-HFET by partially etching the AlGaN barrier layer under the gate, as shown in Figure 4. A larger drain current ($I_{\rm d}$) is obtained in the BGA-HFET owing to the high-concentration 3DEG in the positive-graded AlGaN. The formula for g_m is expressed by

$$g_m = \frac{Z\mu_n C_{\rm OX}}{L_{\rm CH}} V_{DS}, \tag{1}$$

where $L_{\rm CH}$ is the channel length and Z is the channel width. The effective channel length of the BGA-HFET is 0.1 μm (i.e., the length of controlled hole layer in the negative-graded AlGaN, similar to the inversion-layer channel length of the p-body in Si MOSFET) while that of the PolFET and Con-HFET are 0.5 μm (the gate lateral length), which results in the g_m of BGA-HFET being much higher than that of the other two devices according to formula (1). The *I*-*V* output characteristic curves are shown in Figure 7. By integration, the electrons sheet density of the BGA-HFET, PolFET, and Con-HFET are 1.17×10^{13}, 1.23×10^{13}, and 5.07×10^{12} cm^{-2} (which determine the drift region resistance of the power devices), respectively. Consequently, the saturation drain current ($I_{\rm d,sat}$) of the BGA-HFET is increased by 103.5% in comparison with that of the Con-HFET, whereas it has a slight decrease compared with that of the PolFET owing to the depletion effect between the 3DHG and 3DEG in the positive-/negative-graded AlGaN interface. However, the $R_{\rm on,sp}$ (resistance × area) of the BGA-HFET is less than that of the PolFET, because the BGA-HFET is smaller and subsequently its $R_{\rm on,sp}$ is only 0.31 mΩ·cm^2.

Figures 8 and 9 compare the E-field distributions and the 2D equipotential line distributions at breakdown for the three devices. For the BGA-HFET, the depletion region is extended to the drain and the *X*-component of the E-field (E_X) strength is obviously enhanced owing to the assisted depletion effect caused by the polarization junction. Thus, a uniform equipotential line distribution is achieved, as shown in Figure 9. The source causes a new E-field peak (P) and further optimizes the E-field distribution of the drift region. Additionally, the positive and negative polarization charges maintain the charge balance, and almost all of the electric flux from the positive polarization charges terminate at the negative polar-

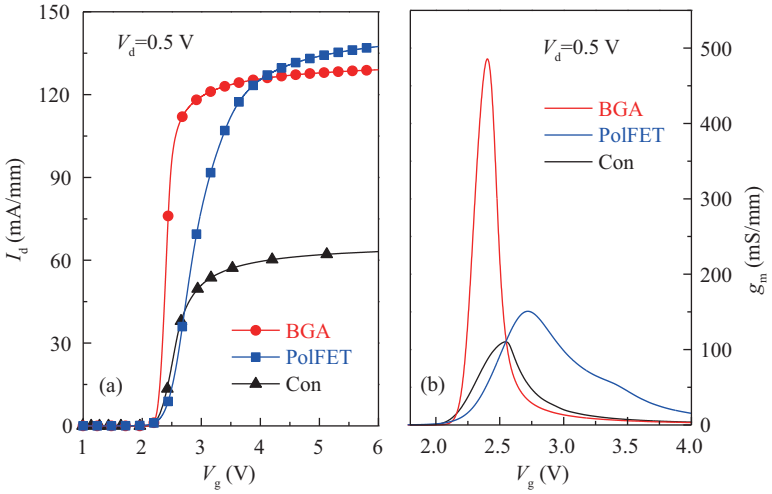

Figure 6 (Color online) (a) Transfer characteristics curves at $V_{\rm d} = 0.5$ V; (b) transconductance at $V_{\rm d} = 0.5$ V.

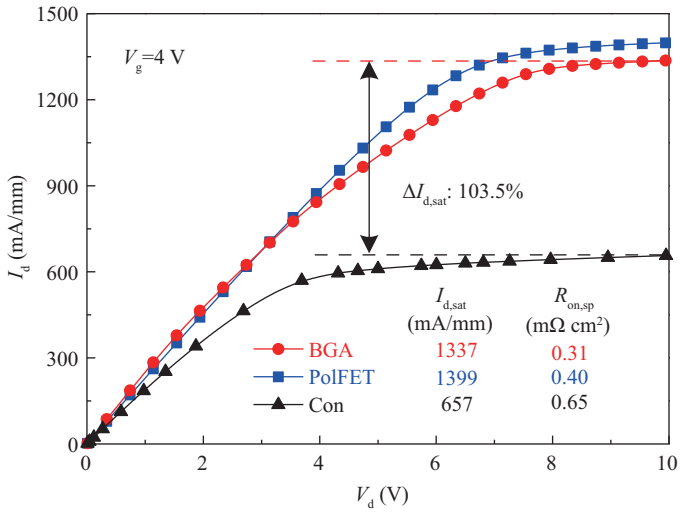

Figure 7 (Color online) I-V output characteristic curves at $V_{\rm g} = 4$ V.

ization charges in the off-state, as shown in Figure 1(c). The back-to-back graded AlGaN resembles an SJ structure [26]. Therefore, the Y-component of the E-field (E_Y) strength is also enhanced, as illustrated in the inset of Figure 8. However, without the SJ-like structure for the PolFET and Con-HFET, the drift region cannot be fully depleted and almost all of the equipotential lines are crowded at the right side of the gate. The premature breakdown is caused by the high gate E-field, as shown in Figure 8.

In fact, the carrier profile strongly depends on the Al composition and the thickness of the graded AlGaN. Figure 10 indicates the 3DEG and 3DHG concentration distributions of the BGA-HFET for different $x_{\rm Al}$ and d. When d is fixed at 100 nm, the 3DEG has the highest electron concentration ($\sim 2\times10^{18}$ cm^{-3}) and the widest electron slab at $x_{\rm Al} = 0.4$; subsequently, the concentration and width of the 3DEG decrease with the decrement of $x_{\rm Al}$, as shown in Figure 10(a). Correspondingly, the 3DHG has similar characteristics to the 3DEG, and its width is slightly smaller than that of the 3DEG at the same $x_{\rm Al}$ because of the depletion effect of the GaN-top with slightly doped n-type on the 3DHG. When $x_{\rm Al}$ is fixed at 0.4, as shown in Figure 10(b), the 3DEG and 3DHG concentrations decrease while their covering widths extend as d increases. This indicates that the $x_{\rm Al}$ and d have a strong impact on modulating the carrier profile. In addition, a negligible carrier concentration exists near the positive-/negative-graded AlGaN interface ($Y = 200$ nm) owing to the 3DHG-3DEG depletion effect between them. Undoubtedly, the $V_{\rm th}$ of the BGA-HFET will also be affected by $x_{\rm Al}$ and d, as shown in Figure 11(a), because of the

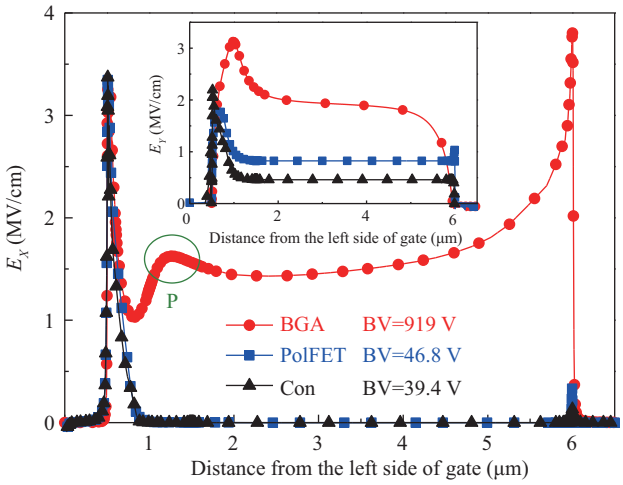

Figure 8 (Color online) E_X and E_Y distributions of the three devices at breakdown (The extracted E-field is located 2 nm below the AlGaN/GaN buffer layer interface, $Y = 302$ nm for BGA-HFET and PolFET, $Y = 227$ nm for Con-HFET).

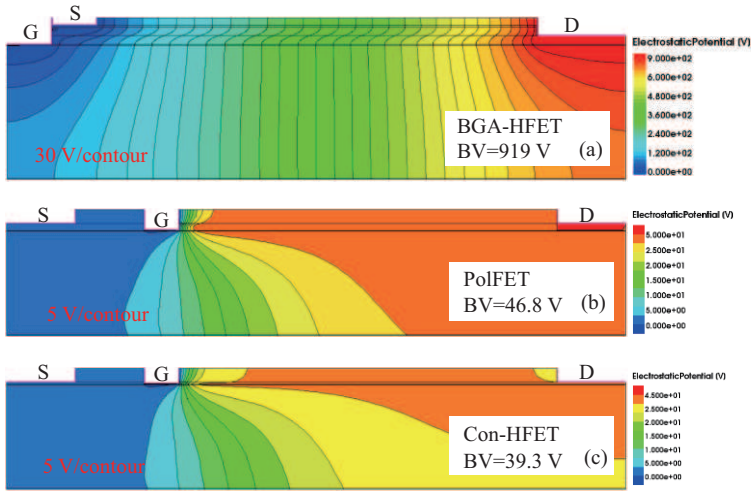

Figure 9 (Color online) 2D equipotential lines distribution of (a) BGA-HFET, (b) PolFET, (c) Con-HFET at breakdown.

variation in the 3DHG concentration, and that x_{Al} has more obvious effects on V_{th}. Figure 11(b) shows the transfer characteristic curves as a function of x_{Al} and d.

Figure 12 illustrates the dependence of the BV and $I_{\mathrm{d,sat}}$ on x_{Al} and d, where the BV is defined as the drain-source voltage at $I_{\mathrm{d}} = 1$ mA/mm under $V_{\mathrm{g}} = 0$ V. The BV increases from 804 to 919 V as x_{Al} increases from 0.2 to 0.4 because the assisted depletion effect of the polarization junction is enhanced. Meanwhile, the $I_{\mathrm{d,sat}}$ also increases from 645 to 1411 mA/mm owing to the significant increment of the 3DEG sheet density. Figure 13 demonstrates the E_X-field distributions at x_{Al}=0.2 and 0.4; it clearly shows that a higher average E_X-field strength is achieved for a higher x_{Al}, leading to a higher BV. The inset in Figure 13 shows the I-V output characteristic curves for different x_{Al}. However, the 3DEG and 3DHG sheet densities maintained although d increased from 70 to 100 nm. This yields the almost constant BV and $I_{\mathrm{d,sat}}$, as shown by red lines in Figure 12.

The analysis above shows that the performances of the BGA-HFET have a certain improvement by increasing x_{Al} and d, especially x_{Al}. However, too high an Al composition may cause a lattice mismatch in the positive-/negative-graded AlGaN layers, and a thick-graded AlGaN layer will increase the process cost. Consequently, the maximum values of x_{Al} and d discussed herein are 0.4 and 100 nm, respectively.

The N region under the source can regulate V_{th} by changing the doping concentration N_{s}. Figure 14 indicates the influence of N_{s} on the V_{th} of the BGA-HFET ($d = 100$ nm, $x_{\mathrm{Al}} = 0.4$). With N_{s} increasing from 8×10^{16} to 2×10^{18} cm^{-3}, V_{th} decreases from 2.19 to 1.66 V because the height of the conduction

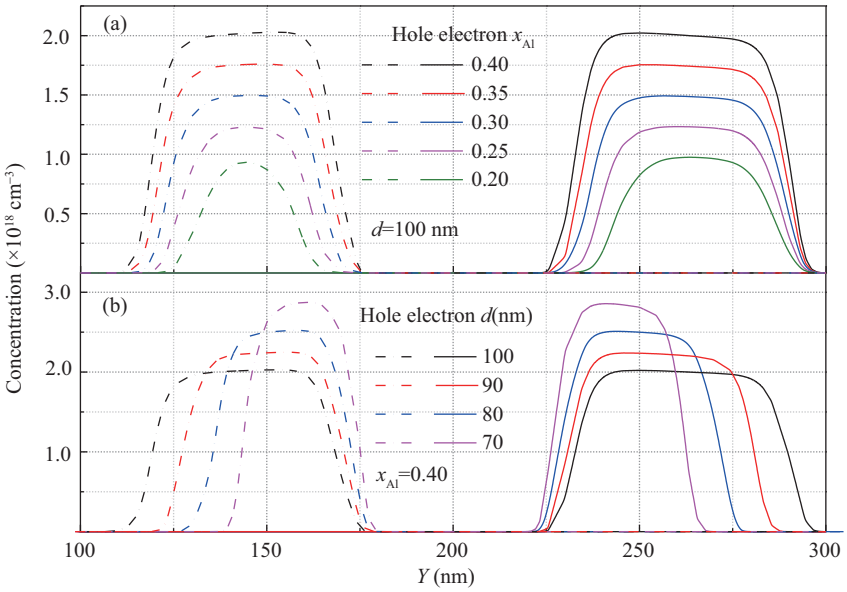

Figure 10 (Color online) 3DEG and 3DHG concentration distributions of BGA-HFET for different (a) x_{Al} and (b) d.

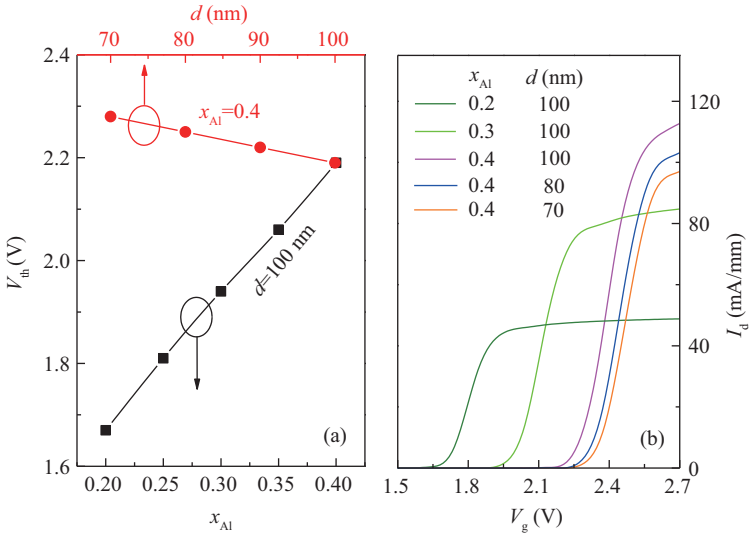

Figure 11 (Color online) (a) Influence of the x_{Al} and d on V_{th}; (b) transfer curves as a function of x_{Al} and d.

band along the gate sidewall is lowered. The inset in Figure 14 shows the transfer curves as a function of N_{s}.

Figure 15 shows the primary fabrication process steps of the BGA-HFET. The process starts with a mesa isolation, implemented by a high-power inductively coupled plasma (ICP) etching. Subsequently, the isolation gap and drain contact region are performed together by low-power ICP etching (Figure 15(b)). Si ions are implanted as the N region under the source to regulate the V_{th}, as shown in Figure 15(c). Next, the Ti/Al/Ni/Au Ohmic contact is formed followed by the plasma-enhanced chemical vapor deposition (PECVD) of Si_3N_4 as the passivation layer and the protection layer of the Ohmic contact (Figure 15(d) and (e)). Subsequently, a 10-nm HfO_2 layer is deposited by atomic layer deposition (ALD) as the gate dielectric after the gate recess formation by low-power ICP etching (Figure 15(f) and (g)). Finally, the device is finished with the source and drain via opening and interconnection after the Ni/Au metal gate deposition. The primary steps are explained above and some process flows are omitted for brevity (annealing, removing mask, etc.).

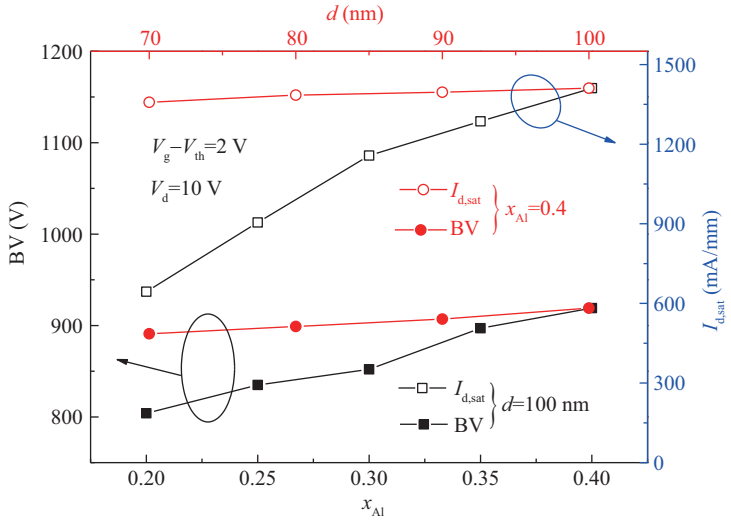

Figure 12 (Color online) Dependence of the BV and $I_{\mathrm{d,sat}}$ on the x_{Al} and d.

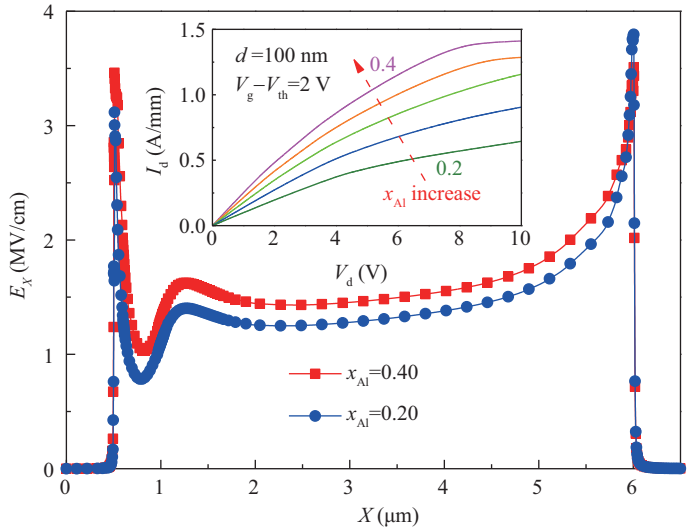

Figure 13 (Color online) E_X distributions ($Y = 302$ nm) and I-V output characteristic curves for different x_{Al}.

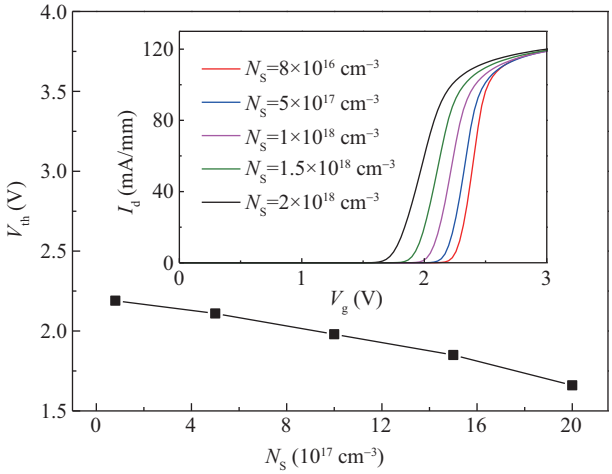

Figure 14 (Color online) Influence of the N_{s} on V_{th} and transfer curves as a function of N_{s}.

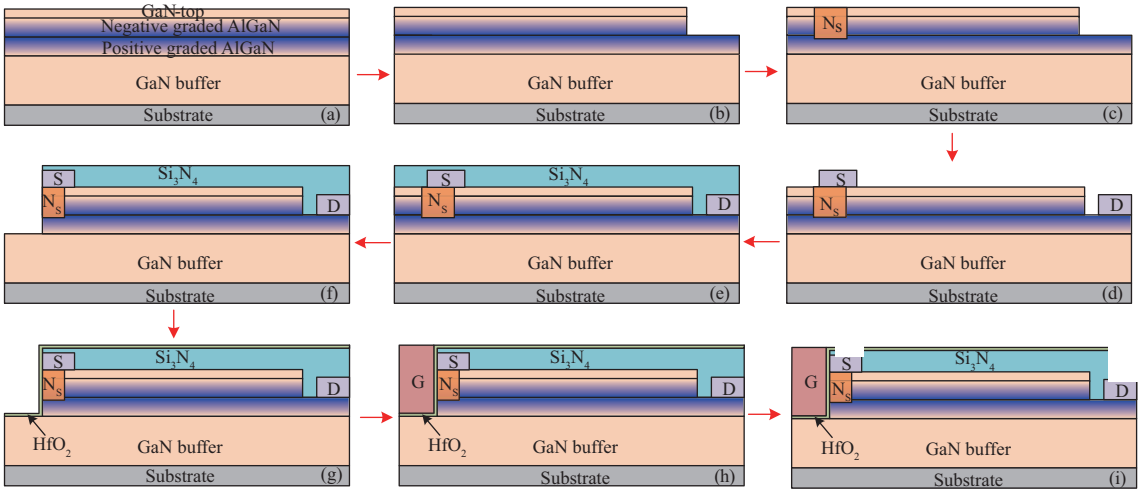

Figure 15 (Color online) Fabrication process for the BGA-HFET structure. (a) Mesa isolation; (b) isolation gap and drain contact region formation; (c) implantation for N region under the source; (d) Ohmic contact formation; (e) PECVD Si_3N_4; (f) gate recess formation; (g) HfO_2 deposition; (h) gate metal formation; (i) source and drain via opening and interconnection.

4 Conclusion

A novel 3DHG E-mode HFET with back-to-back graded AlGaN is proposed and investigated. The 3DEG and 3DHG are induced in the back-to-back graded AlGaN owing to the polarization gradient, and the E-mode is realized because the 3DHG blocks the vertical conductive channel. In the on-state, a large saturation drain current is obtained owing to the high concentration 3DEG in the positive-graded AlGaN. In the off-state, a uniform E-field distribution is achieved owing to the assisted depletion effect by the polarization junction; therefore, the BV of the BGA-HFET is significantly improved. The proposed device significantly enhances the $I_{d,sat}$ and the BV simultaneously, and the technique is available to achieve E-mode GaN power devices of high voltage and high output power.

Acknowledgements This work was supported in part by National Natural Science Foundation of China (Grant Nos. 51677021, 61234006), National Defense Science and Technology Project Foundation of China (Grant No. 1100395), and Fundamental Research Funds for the Central Universities (Grant No. ZYGX2014Z006).

References

1 Chow T P, Tyagi R. Wide bandgap compound semiconductors for superior high-voltage unipolar power devices. IEEE Trans Electron Dev, 1994, 41: 1481–1483
2 Mishra U K, Parikh P, Wu Y-F. AlGaN/GaN HEMTs-an overview of device operation and applications. Proc IEEE, 2002, 90: 1022–1031
3 Micovic M, Kurdoghlian A, Hashimoto P, et al. GaN HFET for W-band power applications. In: Proceedings of the International Electron Devices Meeting (IEDM), San Francisco, 2006. 425–427
4 Zhou Q, Chen W J, Liu S H, et al. Schottky-contact technology in InAlN/GaN HEMTs for breakdown voltage improvement. IEEE Trans Electron Dev, 2013, 60: 1075–1081
5 Ambacher O, Smart J, Shealy J R, et al. Two-dimensional electron gases induced by spontaneous and piezoelectric polarization charges in N- and Ga-face AlGaN/GaN heterostructures. J Appl Phys, 1999, 85: 3222–3233
6 Ohmaki Y, Tanimoto M, Akamatsu S, et al. Enhancement-mode AlGaN/AlN/GaN high electron mobility transistor with low on-state resistance and high breakdown voltage. Jpn J Appl Phys, 2006, 45: L1168–L1170
7 Saito W, Takada Y, Kuraguchi M, et al. Recessed-gate structure approach toward normally off high-voltage AlGaN/GaN HEMT for power electronics applications. IEEE Trans Electron Dev, 2006, 53: 356–362
8 Uemoto Y, Hikita M, Ueno H, et al. A normally-off AlGaN/GaN transistor with $R_{on}A$=2.6 mΩ·cm^2 and BV_{ds}=640 V using conductivity modulation. In: Proceedings of the International Electron Devices Meeting (IEDM), San Francisco, 2006. 1–4
9 Cai Y, Zhou Y G, Chen K J, et al. High-performance enhancement-mode AlGaN/GaN HEMTs using fluoride-based plasma treatment. IEEE Electron Dev Lett, 2005, 26: 435–437
10 Xiong J Y, Yang C, Wei J, et al. Novel high voltage RESURF AlGaN/GaN HEMT with charged buffer layer. Sci China Inf Sci, 2016, 59: 042410

11 Kim K W, Jung S D, Kim D S, et al. Effects of TMAH treatment on device performance of normally off Al_2O_3/GaN MOSFET. IEEE Electron Dev Lett, 2011, 32: 1376–1378
12 Saito W, Omura I, Ogura T, et al. Theoretical limit estimation of lateral wide band-gap semiconductor power-switching device. Solid-State Electron, 2004, 48: 1555–1562
13 Lee J G, Lee H J, Cha H Y, et al. Field plated AlGaN/GaN-on-Si HEMTs for high voltage switching applications. J Korean Phy Soc, 2011, 59: 2297–2300
14 Karmalkar S, Deng J Y, Shur M S. RESURF AlGaN/GaN HEMT for high voltage power switching. IEEE Electron Dev Lett, 2001, 22: 373–375
15 Nakajima A, Sumida Y, Dhyani M H, et al. GaN-based super heterojunction field effect transistors using the polarization junction concept. IEEE Electron Dev Lett, 2011, 32: 542–544
16 Yang C, Xiong J Y, Wei J, et al. Analytical model and new structure of the enhancement-mode polarization-junction HEMT with vertical conduction channel. Superlattices Microstruct, 2016, 92: 92–99
17 Jena D, Heikman S, Green D, et al. Realization of wide electron slabs by polarization bulk doping in graded III-V nitride semiconductor alloys. Appl Phys Lett, 2002, 81: 4395–4397
18 Rajan S, Xing H, DenBaars S, et al. AlGaN/GaN polarization-doped field-effect transistor for microwave power applications. Appl Phys Lett, 2004, 84: 1591–1593
19 Simon J, Wang A K, Xing H, et al. Carrier transport and confinement in polarization-induced three-dimensional electron slabs: importance of alloy scattering in AlGaN. Appl Phys Lett, 2006, 88: 042109
20 Simon J, Protasenko V, Lian C X, et al. Polarization-induced hole doping in wide-band-gap uniaxial semiconductor heterostructures. Science, 2010, 327: 60–64
21 Li S B, Ware M, Wu J, et al. Polarization induced pn-junction without dopant in graded AlGaN coherently strained on GaN. Appl Phys Lett, 2012, 101: 122103
22 Fang Y L, Feng Z H, Yin J Y, et al. AlGaN/GaN polarization-doped field-effect transistors with graded heterostructure. IEEE Trans Electron Dev, 2014, 61: 4084–4089
23 Zhou X Y, Feng Z H, Fang Y L, et al. Simulation study of GaN-based HFETs with graded AlGaN barrier. Solid-State Electron, 2015, 109: 90–94
24 Luo X R, Peng F, Yang C, et al. Polarization-doped enhancement mode HEMT. US Patent, US15/623371, 2017-6-14
25 Appels J A, Vaes H M J. High voltage thin layer device (RESURF devices). In: Proceedings of the International Electron Devices Meeting (IEDM), Washington, 1979. 238–241
26 Chen X B, Sin J K O. Optimization of the specific on-resistance of the COOLMOS. IEEE Trans Electron Dev, 2001, 48: 344–348
27 Zhang L, Ding K, Yan J C, et al. Three-dimensional hole gas induced by polarization in (0001)-oriented metal-face III-nitride structure. Appl Phys Lett, 2010, 97: 062103
28 Li L, Yang L A, Cao R T, et al. Reduction of threading dislocations in N-polar GaN using a pseudomorphicaly grown graded-Al-fraction AlGaN interlayer. J Cryst Growth, 2013, 387: 1–5
29 Uren M J, Nash K J, Balmer R S, et al. Punch-through in short-channel AlGaN/GaN HFETs. IEEE Trans Electron Dev, 2006, 53: 395–398
30 Wei J, Jiang H P, Jiang Q M, et al. Proposal of a GaN/SiC hybrid field-effect transistor for power switching applications. IEEE Trans Electron Dev, 2016, 63: 2469–2473